

AperTO - Archivio Istituzionale Open Access dell'Università di Torino

Peroxide-driven catalysis of the heme domain of *A. radioresistens* cytochrome P450 116B5 for sustainable aromatic rings oxidation and drug metabolites production

This is the author's manuscript

Original Citation:

Availability:

This version is available <http://hdl.handle.net/2318/1727623> since 2020-02-18T11:50:21Z

Published version:

DOI:10.1016/j.nbt.2019.08.005

Terms of use:

Open Access

Anyone can freely access the full text of works made available as "Open Access". Works made available under a Creative Commons license can be used according to the terms and conditions of said license. Use of all other works requires consent of the right holder (author or publisher) if not exempted from copyright protection by the applicable law.

(Article begins on next page)

This is the author's final version of the contribution published as:

Peroxide-driven catalysis of the heme domain of *A. radioresistens* cytochrome P450 116B5 for sustainable aromatic rings oxidation and drug metabolites production

Alberto Ciaramella, Gianluca Catucci, Giovanna Di Nardo, Sheila J. Sadeghi
and Gianfranco Gilardi*

The publisher's version is available at:

<https://www.sciencedirect.com>

When citing, please refer to the published version.

Link to this full text:

<https://www.sciencedirect.com/science/article/pii/S187167841831834X>

This full text was downloaded from iris-AperTO: <https://iris.unito.it/>

Peroxide-driven catalysis of the heme domain of *A. radioresistens* cytochrome P450 116B5 for sustainable aromatic rings oxidation and drug metabolites production

Alberto Ciaramella, Gianluca Catucci, Giovanna Di Nardo, Sheila J. Sadeghi
and Gianfranco Gilardi*

Department of Life Sciences and Systems Biology,
University of Torino, Via Accademia Albertina 13, 10123 Torino, Italy.

* Address correspondence to:

Gianfranco Gilardi
gianfranco.gilardi@unito.it

Abstract

The heme domain of cytochrome P450 116B5 from *Acinetobacter radioresistens* (P450 116B5hd), a self-sufficient class VII P450, was functionally expressed in *Escherichia coli*, purified and characterised in active form. Its unusually high reduction potential (-144 ± 42 mV) and stability in the presence of hydrogen peroxide make this enzyme a good candidate for driving catalysis with the so-called peroxide shunt, avoiding the need for a reductase and the expensive cofactor NAD(P)H. The enzyme is able to carry out the peroxide-driven hydroxylation of aromatic compounds such as *p*-nitrophenol ($K_M = 128.85 \pm 29.51$ μM and $k_{\text{cat}} = 2.65 \pm 0.14$ min^{-1}), 10-acetyl-3,7-dihydroxyphenoxazine ($K_M = 6.01 \pm 0.32$ μM and $k_{\text{cat}} = 0.33 \pm 0.03$ min^{-1}), and 3,5,3',5'-tetramethylbenzidine (TMB). Moreover, it catalyses different reactions on well-known drugs such as hydroxylation of diclofenac ($K_M = 49.60 \pm 6.30$ μM and $k_{\text{cat}} = 0.06 \pm 0.01$ min^{-1}) and N-desmethylation of tamoxifen ($K_M = 57.20 \pm 7.90$ μM and $k_{\text{cat}} = 0.79 \pm 0.04$ min^{-1}). The data demonstrate that P450 116B5hd is an efficient biocatalyst for sustainable applications in bioremediation and human drug metabolite production.

Keywords

P450; Human P450 substrates; Peroxide shunt; Peroxygenase activity; diclofenac; tamoxifen

Abbreviations

P450 116B5hd: cytochrome P450 116B5 heme domain; KPi: Phosphate buffer; HRP horseradish peroxidase; P450: cytochrome P450; HD: heme domain; NAD(P)H: β -nicotinamide adenine dinucleotide (phosphate) reduced; *p*-NP: para-nitrophenol; ϵ : molar extinction coefficient; TMB: 3,5,3',5'-tetramethylbenzidine; SDT: sodium dithionite; Amplex Red: 10-acetyl-3,7-dihydroxyphenoxazine; P450BS β : fatty acid K- or L-hydroxylating-cytochrome P450 from *Bacillus subtilis*; 5'OHD: 5' hydroxydiclofenac; δ ALA: aminolevulinic acid; IPTG isopropyl β -D-1-thiogalactopyranoside; UPOs unspecific peroxygenase (EC 1.11.2.1); DSC: Differential scanning calorimetry; DLS: Dynamic light scattering.

Introduction

Cytochromes P450 are widely distributed heme thiolate monooxygenases, characterised by a typical absorbance peak at 450 nm when the heme is reduced and complexed with carbon monoxide (CO) [1]. They catalyse a variety of regio- and stereo-selective reactions on a wide range of substrates, including xenobiotic compounds, steroids, chemicals, pharmaceuticals and environmental pollutants, making them attractive targets for biocatalysis and green chemistry applications [2]. Despite the importance and versatility of these reactions, most membrane-bound mammalian P450s are not exploitable as biocatalysts because of their low stability and poor catalytic efficiency [3]. One of the most studied bacterial P450s is the catalytically self-sufficient P450 102A1 from *Bacillus megaterium*, also known as cytochrome P450 BM3 [4]. It is a natural fusion of the P450 domain with its redox partner, a mammalian-like di-flavin reductase, with FAD-FMN as cofactors. This soluble enzyme is not only a good model for mammalian P450s [5], but also a genuine biocatalyst due to its efficient catalytic self-sufficiency. To date, very few self-sufficient P450s have been described [2]. Different kinds of artificial fusion proteins have also been designed through protein engineering by rational design, including the so-called “molecular Lego” approach, as well as directed evolution [6,7]. Although the self-sufficiency is certainly a great advantage in using these enzymes, it does not circumvent the need for expensive NAD(P)H. One strategy successfully applied is the use of whole-cell systems [8,9] where the NADPH is supplied endogenously by the cells. A more practical approach is the use of the peroxide-shunt, in which hydrogen peroxide (H₂O₂) is the source of both oxygen and reducing power, leading directly to the highly reactive compound I species [10]. This has been demonstrated for the CYP152 subfamily that includes P450_{SP} [11], P450_{BS} [12] and P450_{CLA} [13]. As they catalyse exclusively the hydroxylation of long-chain fatty acids with high specificity, some strategies have been applied to extend their substrate recognition using point mutagenesis or decoy-molecules [14,15]. However, the use of hydrogen peroxide to drive P450 reactions has the disadvantage of destabilising the enzyme structure.

Here, the characterization is reported of the heme domain of cytochrome P450 116B5 (P450 116B5hd), initially isolated from *A. radioresistens* growing on medium and long chain alkanes [16]. Its catalytic activity with a range of aromatic compounds and two drugs is demonstrated, using H₂O₂ as source of electrons. The choice of these substrates was motivated by the fact that *A. radioresistens* is known to be able to

mineralise aromatic compounds [17] and attack the imipenem ring involved in drug resistance phenomena [18]. The use of peroxide rather than NAD(P)H can overcome the limitation already reported for other full-length P450 116B enzymes [19, 20].

Materials and Methods

All the reagents and standards used were from Sigma Aldrich (MO, USA) and Carlo Erba (Italy). Plasmid sequencing was carried out by Eurofins Genomics (Germany).

Gene sub-cloning

P450 116B5hd was sub-cloned between EcoRI and NdeI restriction sites in a pET-30a (+) vector (EMD Biosciences). The same 5'-3' forward primer (GGAATTCCATATGCATCATCACCATCACCACAAC) was used for the PCR amplification of all the heme domain constructs. The reverse primers CGGAATTCTTACGGCGCTCCAATAGGAAAAGTGG, CGGAATTCTTAGTTGCCACTCAGTCCACAAGC, and CCGGAATTCTTACGGACGGGTCATCGCTTTA were used for the amplification of the 442, 424 and 450 amino acid (aa) constructs, respectively. A boundary domain analysis was carried out to determine the best position for primer design. Secondary structure as well as a boundary bond prediction was obtained using PSIPRED II server [21]. An N-terminal 6xHis tag was added to all the constructs and the correct amino acid sequence was confirmed by sequencing of the insert.

P450 116B5hd expression and purification

E. coli BL21 (DE3) was transformed with the pET116B5hd plasmid (N-terminal 6x His Tag) and expression of the protein carried out for 24h in LB medium supplemented with 0.5 mM of δ -aminolevulinic acid (δ Ala) and 100 μ M IPTG. Cells were subsequently harvested by centrifugation at 4°C, then resuspended and sonicated (5 \times 30 s pulses with a Misonix Ultrasonic Sonicator, Teltow, Germany) in 50 mM KPi pH 6.8 buffer supplemented with 100 mM KCl, 1 mg/mL lysozyme, 1% Triton X-100 and 1 mM PMSF (phenylmethylsulfonyl fluoride), and 1 mM benzamidine. The lysate was loaded onto a 1 ml nickel-ion affinity column (His-trap HP, GE Healthcare) and eluted applying a linear gradient of imidazole from 20 to 200 mM. This was followed by size exclusion chromatography (SEC) in 50 mM KPi pH 6.8, 200 mM KCl. The purified protein was stored

in 50 mM KPi pH 6.8, 10% glycerol. The monomeric and dimeric forms were separated into two peaks extrapolated from a calibration curve obtained with cytochrome c (12.4 kDa), albumin (66 kDa), glucose oxidase (130 kDa) and apoferritin (430 kDa) as molecular weight standards. Protein purity was assessed by SDS-Polyacrylamide gel electrophoresis (PAGE). The concentration of the folded protein was evaluated from the cytochrome P450-CO complex spectrum upon reduction with sodium dithionite and CO bubbling of the protein sample using an extinction coefficient of $91000 \text{ M}^{-1} \text{ cm}^{-1}$ [1]. P450 BM3 and its isolated heme domain BMP were also used in catalysis experiments for comparison with P450 116B5hd. P450 BM3 and BMP were expressed in *E. coli* BL21(DE3) cells transformed with the pT7BM3Z and pETBMP plasmids, respectively and subsequently used for the purification of the enzymes according to the method described in [22].

Differential scanning calorimetry (DSC)

DSC was carried out using a Microcal VP-DSC instrument (Malvern) with a temperature gradient of 25-90°C, a scan rate of 90°C/h and 10 min. of pre-scan equilibration [23]. The experimental data were analysed using Microcal Origin software. In order to assess the best conditions in terms of protein stability, phosphate, tris-HCl or citrate buffers with different amounts of KCl (to maintain the ionic strength constant at different pH values from 5.0 to 8.0) were tested. All buffers were degassed, contained 10% glycerol and were used also for reference scans. All samples were run using 10 μM enzyme.

Dynamic light scattering (DLS)

The purified protein (10 μM) in 30 μl of filtered 50 mM KPi buffer pH 6.8, was analyzed in a Zetasizer nano ZS90 (Malvern) at 25°C. The measurement range was fixed between 0.3 nm and 5.0 microns (diameter). The average size of the particles in solution was calculated from three technical replicates.

Titration experiments of potential substrates and inhibitors

Spectral binding titrations were performed to determine the dissociation constants (K_D) for different substrates. Aliquots of substrate or inhibitor (0.5–1.0 μL) were added from stock solutions (10-100 μM) in phosphate buffer or ethanol (max 1% of final volume) to 2.0 μM P450 116B5hd in 50 mM KPi pH 6.8, 10% glycerol. The apparent K_D was obtained by fitting the data points to the hyperbolic equation $\Delta A = B_{\text{max}}S / (K_D S)$, where S represents substrate concentration, K_D is the spectral dissociation constant, and B_{max} is

the maximal binding. All spectra were recorded at 25°C.

Reduction potential determination

Spectro-electrochemical experiments were carried out at 25°C in a glovebox (Belle Technology, Weymouth, UK) under a nitrogen atmosphere to ensure anaerobic conditions using an Ag/AgCl reference electrode and a laminar gold working electrode. Sodium dithionite was titrated in aliquots of 0.5 µL using a 0.5 mM stock solution and allowed to equilibrate for at least 5 min. Protein and sodium dithionite solutions were prepared in 50 mM KPi pH 6.8 buffer. Methylene blue (+11 mV), O-safranin (-280 mV), phenazine methosulfate (+80 mV), anthraquinone-2,6-disulfonic acid (-185 mV), benzyl viologen (-359 mV) and methyl viologen(-440mV) were added to the solution as electron mediators. The concentration of mediator was held at <0.1 µM to avoid interference in the spectrum recorded. Benzyl viologen and methyl viologen stocks were prepared in water. All other redox mediators were diluted in methanol to a final concentration of 5 mM. Then a 1:100 dilution of each mediator was prepared using the storage buffer. Finally, the protein solution was mixed with the mediators. The spectra of the Soret peaks reflecting Fe³⁺/Fe²⁺ transitions were recorded after each addition. The midpoint potentials were obtained by plotting the percentage of reduced fraction of the protein (calculated using the absorbance values at 550 nm) versus the potential and fitted to the Nernst equation.

Spectroscopic evaluation of hydrogen peroxide tolerance

The enzyme was incubated with increasing concentrations of H₂O₂ (0.25 to 5 mM) for 30 min, taking a measurement every 30 s using an Agilent 8453 UV-Vis spectrophotometer (diode array) at the controlled temperature of 15°C (Peltier Agilent 89090 A). P450 116B5hd was used at a concentration of 2.5 µM in 50 mM KPi pH 6.8. All buffers also contained 10% glycerol. BMP was used as a reference protein, and the measurements were performed at the same enzyme concentration in a 100 mM KPi pH 8, 1 mM DTT. The Soret peak intensity (419-420 nm) was plotted as a function of time and fitted to a single exponential decay function to obtain the rate constant value k.

Catalytic assays

Catalysis measurements in solution were performed preparing 400 µL of reaction mixtures containing 1 µM or 500 nM of P450 116B5hd in 50 mM potassium phosphate, pH 6.8. The

reactions were initiated with the addition of H₂O₂ in the concentration range 0.2 to 1 mM. Control reactions were always performed in the absence of H₂O₂ and the absence of the enzyme to exclude the direct oxidation of the substrate by H₂O₂.

Incubations with different concentration of *p*-nitrophenol were carried out for 30 min at 30°C. The Michaelis-Menten curve was built using 500 nM enzyme, 2 mM H₂O₂ and 50 to 1600 μM of *p*-nitrophenol. 1% trichloroacetic acid (TCA) was added to terminate the reaction. Samples were then centrifuged for 5 min at 10,000 xg and the supernatant was transferred to a clean tube. Colour development was achieved by adding 40 μl of 9M NaOH. The *p*-nitrocatechol product was quantified spectrophotometrically within 10 min (after the reaction had been terminated) by measuring the absorbance at 515 nm, in a microplate reader using an ϵ of 12.4 mM⁻¹ cm⁻¹ [24]. The conversion of *p*-nitrophenol was also evaluated as a function of time. The experiment was performed in 50 mM Kpi pH6.8 at 30°C. The enzyme (1 μM) was incubated with 0.6 mM of *p*-nitrophenol and the reaction started with 0.6 mM H₂O₂. Aliquots of reaction mixture were collected at 5, 15, 45, 60, 90 min and the enzyme was inactivated with 30% TCA. Colour recovery and product quantification were obtained as described above.

For Amplex red and TMB catalytic assays, P450 116B5hd was used at a different concentration ranging from 0.5 to 10 μM while the substrate was kept at the constant concentration of 100 μM. To test the presence of products, the reaction was initiated with 0.5 mM H₂O₂. A working solution containing 100 μM Amplex red or TMB and 50 mM KPi pH 6.8 was prepared immediately before use from the stock solutions (above). Aliquots of each enzyme concentration were pipetted in NUNC96 96-well microplates (Thermo Fisher, MA, USA) with 100 μL volume of working solution and initiated with addition of 0.5 mM H₂O₂. Absorbance measurements at 570 nm or 455 nm were made using a SPECTROstar nano microplate reader (BMGLabtech, UK) to detect the products. Controls were performed in the absence of the enzyme or H₂O₂. The kinetic parameters were extrapolated from a Michaelis-Menten curve obtained with increasing concentration of an Amplex red standard and a fixed concentration of enzyme (0.5 μM) and H₂O₂ (0.5 mM) incubated for 30 min at 30°C.

Drug metabolite production

The reaction mixture comprised 1-2 μM enzyme, 0.5 mM H_2O_2 and a specified amount of the substrates in 50 mM potassium phosphate buffer (pH 6.8). After a pre-incubation of 5 min at 30°C, the reactions were initiated by the addition of H_2O_2 and monitored for up to 30 min. HPLC analysis of tamoxifen and diclofenac metabolites was performed with an HPLC coupled with a diode array UV detector (Agilent-1200, Agilent technologies, CA, USA) set at 240 and 276 nm, respectively after 30 min incubation at 30°C in 50 mM KPi pH 6.8. The reactions were terminated with cold acetonitrile in a 3:1 ratio, mixed and centrifuged at 13,000 $\times g$ value for 5 min. The supernatant was separated and 30 μL of mixture were injected into the HPLC column. A C18 prepacked column (Phenomenex-Kinetex Core Shell) was used for the chromatographic separation using 60-40% acetonitrile -0.1% formic acid as the mobile phase [25].

Results and discussion

Sub-cloning, expression and characterisation of P450 116B5hd

Cytochrome P450 116B5 consists of a P450 heme domain naturally fused to PFOR reductase, that in turn contains one 2Fe-2S and one FMN domain [16]. This makes cytochrome P450 116B5 a self-sufficient enzyme since only NADPH is required to perform catalysis as electrons are passed from NADPH to the 2Fe-2S domain first, then to the FMN that sustains the catalysis by the heme domain. In order to engineer a heme domain clone (P450 116B5hd) for expression in *E.coli*, a secondary structure prediction was performed using the PsiPred server [21] based on the crystal structure of the homologous cytochrome P450 116B46 (6GII) [26] with an identity of 55% (**Figure 1A**). The results indicated that the linker region between the PFOR reductase and the heme domain consists of residues 421-450. Three different constructs were designed, amplified from the full-length clone and ligated into a pET-30a(+) vector for expression. They contained a short (424 aa), medium (442 aa) or long (450 aa) final coil (His tag excluded) as shown in Figure 1B. Preliminary small-scale expression of the 442 aa construct showed a higher level of expression in the soluble fraction for this protein, which was therefore chosen for further studies. Expression was performed in *E. coli* BL21 (DE3) and purification was carried out on a nickel column followed by a size exclusion chromatography column that led to a major single band at about 50 kDa on SDS-PAGE consistent with the predicted molecular mass of 51,694 Da (His-tag included) (Figure 1C). The purity expressed as the

A_{419}/A_{280} ratio was found to be in the range of 1.18 to 1.30 . The polydispersity index determined by dynamic light scattering (DLS) was found to decrease after SEC step due to the reduction of the amount of aggregated protein.

The UV-visible absorption spectrum of the pure protein in its oxidized form shows the typical Soret peak at 419 nm and two Q bands at 539 and 573 nm, respectively. When reduced with sodium dithionite the Soret peak shifts to 410-411 nm, while a single peak appears at 550 nm. The typical reduced and CO-bound form appears at 450 nm after bubbling with CO (**Figure 2A**). This absorption band is used to calculate the concentration of the active enzyme using an extinction coefficient of $91000 \text{ M}^{-1} \text{ cm}^{-1}$ [1].

DLS was used to determine the size of the main protein band (90-92%) eluted from a SEC column in 50 mM KPi pH 6.8, 200 mM KCl. This value was found to be 7.57 ± 1.10 nm in diameter and consistent with the monomeric form of the enzyme according to the calibration curve (Supplementary Figure S1). A minor peak (8-10%) was eluted before the main peak on SEC and was assigned to a dimeric form of the protein according to the calibration curve.

Differential scanning calorimetry (DSC) was used to follow the thermal unfolding process at different pH values in 50 mM KPi containing 10% glycerol, maintaining a constant ionic strength. Data showed two underlying transitions at pH 5.0-5.5 and pH 8.0, while only one was present in the pH range 6.2-7.4 (**Figure 3A, Table 1**). The appearance of two transitions is explained by the presence of mixed populations of enzyme in solution at these extreme pH values. In contrast, at pH 6.8, the enzyme showed only one transition with a T_M of 48.2°C , which also has the highest enthalpy value (502.0 KJ/mol), indicating that this pH offers the best conditions in terms of both protein homogeneity and stability, and was therefore used for the subsequent activity studies.

The catalytic activity of P450 116B5hd was measured using $600 \mu\text{M}$ *p*-nitrophenol as a marker substrate and catalysis was sustained by 0.5 mM of H_2O_2 at different pH values in 50 mM KPi containing 10% glycerol. As shown in Figure 3B, the optimal pH for activity ranged from 6.2 to 6.8, and was in line with the thermal unfolding experiments. For this reason, the storage buffer as well as the activity tests were performed using 50 mM KPi

pH 6.8 with 10% glycerol.

Binding of potential substrates and inhibitors

The low-to-high spin transition of the Soret peak is often used to determine the binding interaction of ligands in the P450 active site. For this reason, a screening of potential inhibitors and substrates was carried out monitoring the shift of the Soret peak at 419 nm to assess if they act as a type I (substrates) or a type II (inhibitors) ligands (**Table 2**). Small shifts in the Soret peak from 419 nm to 416 nm have been reported in the literature for other cytochromes P450 of the same subfamily [27] using a range of monounsaturated fatty acids. Here, similar small blue shifts were observed with a number of monounsaturated fatty acid such as myristoleic and palmitoleic acids (Table 2). The increase at 390-394 nm was not observable, but it can be discerned in the difference spectra allowing for the K_D determination (inset Figure 2). Spectrophotometric determination of binding of *p*-nitrophenol was hindered by the absorbance of this substrate. Two drugs, diclofenac and tamoxifen, were also tested, leading to a small blue shift only in the case of diclofenac.

Nitrogen-containing ligands with different steric hindrance, such as imidazole, histidine, ketoconazole and imazalil, were chosen to test their ability to coordinate the heme iron directly, inducing the typical red (type II) shift. As shown in Table 2 they all resulted in an increased absorption between 425 nm and 435 nm, typical of P450 inhibitors which bind directly to Fe^{3+} and replace the water molecule as the sixth ligand (Figure 2B) [28]. This behaviour can be also due to the binding of nitrogen to the water molecule, as shown in some recent work [29]. Titration with increasing amounts of ligand allowed the determination of the dissociation constants (K_D) of 24 μ M and 671 μ M for ketoconazole and imidazole respectively (Supplementary Figure S2).

These data suggest that P450 116B5hd shows a broad ligand recognition, where even bulky molecules such as ketoconazole can be accommodated in its active site.

Determination of the heme reduction potential

Reduction potentials of the heme were measured via anaerobic spectro-potentiometric titrations [30]. The change in population from the oxidized (Fe^{3+}) to the reduced (Fe^{2+}) form upon addition of sodium dithionite (83 nM aliquots final concentration) was followed

by measurement of the spectral transition related to the merging of the Q-bands into a single band at 550 nm. Reduction potential values were calculated in the absence and presence of ligands (ketoconazole and diclofenac) by plotting the calculated reduced heme fraction *versus* the recorded potential using the Nernst equation (Figure 3C). The resulting values were -144 ± 42 mV in the absence of ligand, -109 ± 9 mV in the presence of the substrate diclofenac and -223 ± 10 mV in the presence of the inhibitor ketoconazole.

These values of potentials are unusually positive when compared to other P450 enzymes [27]. However, they have also been reported for the cytochrome P450 152 sub-family [31] that are H₂O₂ resistant and act as peroxygenases, using H₂O₂ as both reducing agent and oxygen donor. As the reduction potential is the consequence of the environment of the heme iron, it can be inferred that the amino acids surrounding the heme contribute to creating a more stable condition for the Fe to interact with H₂O₂. This leads to a ferric-hydroperoxo form which is then converted into the ferryl-oxo compound I and makes the peroxide shunt more efficient compared to other P450s studied to date.

Stability of P450 116B5hd in the presence of hydrogen peroxide

It has been shown that H₂O₂ can cause oxidative damage to the heme and to the protein, usually involving the oxidation of the heme thiolate ligand to sulfenic acid [32], causing a decrease both in catalytic performance and heme absorbance at 419 nm [33]. Stability assays over time were performed with P450 116B5hd at increasing concentrations of H₂O₂ (from 0.25 to 5 mM) monitoring the absorbance at 419 nm. The heme domain of cytochrome P450 BM3 (BMP) was taken as a reference, as it is known that this enzyme can also function as a peroxygenase [34-36]. The Soret peak was monitored for both enzymes every 30 s over 30 min upon addition of hydrogen peroxide at 15°C (**Figure 4A** and **4B**). Depending on the level of stability, the Soret peak decay curves shown in Figures 4C, D decreased over time, resulting in different rate constants for the two proteins. The rates and amplitude of the decaying signals are reported in Table 3.

Figure 4 clearly shows that P450 116B5hd even at the highest concentration of H₂O₂ (5mM) lost only 10% of the absorbance at 419 nm, while BMP under the same conditions lost 83% of its A₄₁₉. Table 3 shows a clear difference in the trend with a much higher

resistance of P450 116B5hd to H₂O₂ compared to BMP. This is an interesting observation as it suggests that H₂O₂ might support P450 116B5hd catalysis and is stable at the 0.4 mM H₂O₂ concentration chosen for the incubations reported below. Stability to H₂O₂ gives an advantage to enzymes capable of using it during a greater number of turnovers before definitive inactivation, which has been observed even for a very efficient peroxidase such as HRP [37, 38]. In the absence of a 3D structure of the enzyme it is not possible to make a detailed analysis of the amino acid sidechains that surround the heme, but certainly the higher reduction potential measured for P450 116B5hd is a feature shared with the cytochrome P450 152 subfamily that is also stable to H₂O₂ [33].

Hydrogen peroxide driven conversion of *p*-nitrophenol to *p*-nitrocatechol

As it is known that BMP is able to perform catalysis *via* a peroxygenase activity [38], a comparative study was performed between BMP and P450 115B6hd using the full length cytochrome P450 BM3 as control [40]. *p*-Nitrophenol was chosen as substrate because it is converted to *p*-nitrocatechol that can be easily detected after treatment with alkali by reading absorbance at 515 nm. Furthermore, *p*-nitrophenol has been reported as a recognised substrate of BM3 WT [41]. The results shown in **Figure 5** demonstrate that, while catalysis driven by NADPH in P450 BM3 is more efficient than that driven by H₂O₂ in BMP, the H₂O₂- driven catalysis in P450 116B5hd is 38x better than even the best case for P450 BM3 (2.573 versus 0.063 product/minutes/moles of enzyme). The kinetic parameters for P450 116B5hd were calculated and the Michaelis-Menten curve is reported in **Figure 6A**, resulting in a k_{cat} of $2.65 \pm 0.14 \text{ min}^{-1}$ and a K_{M} of $128.85 \pm 29.51 \mu\text{M}$. These data show not only that P450 116B5hd is stable in the presence of H₂O₂, but its catalysis can also be efficiently sustained avoiding the need for the reductase and NADPH.

Catalytic activity of P450 116B5hd towards aromatic compounds and drugs

Owing to the ability of *A. radioresistens* to efficiently grow on aromatic compounds as sole carbon source [17] and given that it has been reported to oxidise synthetic drugs [18,42], P450 116B5hd was incubated with a range of compounds exploiting its peroxygenase activity described above (**Table 4**). In a first instance, chromogenic and fluorescent compounds that give a coloured product when enzymatically hydroxylated or demethylated were screened spectrophotometrically. 10-acetyl-3,7-dihydroxyphenoxazine (Amplex red) and 3,5,3',5'-tetramethylbenzidine (TMB), well known horseradish peroxidase

(HRP) substrates, have been reported to also be substrates of some P450s, such as cytochromes P450 102A1 (BMP) and P450 152A1 (P450_{BSβ}), that convert the substrate Amplex red into resorufin using the peroxide shunt [43], while TMB is oxidised into 3,3',5,5'-tetramethyl-1,1'-bi(cyclohexa-2,5-dien-1-ylidene)-4,4'-diiminium (TMB ox) *via* a fatty acid dependent peroxxygenase mechanism by P450_{BSβ} [44]. Using the peroxide shunt, P450 116B5hd was found to convert both substrates as confirmed by the presence of a peak at 570 nm for resorufin and 455 nm for TMB ox. No conversion was observed in control experiments without enzyme (Supplementary Figure S3). Furthermore, both products were obtained without the addition of further organic solvents or fatty acids, confirming the propensity of this enzyme to convert aromatic compounds directly, without decoy substrate. Both reactions were performed at 30°C for 30 min in the dark. The catalytic oxidation of Amplex red was found to follow a typical Michaelis-Menten kinetic (Figure 6B) from which a k_{cat} of $0.33 \pm 0.03 \text{ min}^{-1}$ and $K_M = 6.01 \pm 0.32 \text{ }\mu\text{M}$ were calculated.

Further experiments were carried out to test the ability of P450 116B5hd to recognise the well-known drugs, tamoxifen and diclofenac. Tamoxifen is a prodrug, currently used for the treatment of breast cancer, gynecomastia and infertility. It has relatively little affinity for its target protein, the estrogen receptor (ER). Its metabolism involves P450 2D6 and P450 3A4 resulting in active metabolites such as 4-hydroxytamoxifen and N-desmethyl-4-hydroxytamoxifen that have 30–100x greater affinity for the ER than tamoxifen itself. Recently, other cytochromes P450 116B were proposed as human drug metabolite producers [19,45]. However, despite an unusually high regio- and stereoselectivity of the reactions catalysed by P450s, and the overall mild reaction conditions compared with organic synthesis, the scale-up of the system remains extremely difficult due to the high uncoupling, low activity and stability of these enzymes. Here, the production of N-desmethyl tamoxifen with P450 116B5hd was followed by HPLC (Supplementary Figure S4) showing typical Michaelis-Menten kinetics (Figure 6C) with a k_{cat} of $0.79 \pm 0.04 \text{ min}^{-1}$ and a K_M of $57.20 \pm 7.90 \text{ min}^{-1}$. The total turnover reached after 30 min ranged from 39 to 59% depending on the substrate. Longer incubations of the enzyme with a fixed substrate concentration did not result in an increase of the product amount, as shown for *p*-nitrophenol (Supplementary Figure S6).

Diclofenac has been reported to be converted into 5-hydroxydiclofenac by cytochrome

P450 116 from different species [19,45]. Since the consistent presence of this drug and its metabolite is of increasing environmental concern, the ability of P450 116B5hd to perform its H₂O₂ driven catalysis was tested. After 30 min incubation with H₂O₂ and 0.5 mM diclofenac, 0.5 μM of P450 116B5hd was found to convert diclofenac into 5-hydroxydiclofenac, monitored by reverse phase HPLC (Supplementary Figure S5), as shown by the appearance of a peak at t_R of 7.99-8.01 min corresponding to the 5-hydroxydiclofenac standard. However, an additional peak at t_R 7.3 min was also found and attributed to diclofenac-2,5-iminoquinone that has been reported to be a byproduct derived from the autoxidation of 5-hydroxydiclofenac [19,46]. It can be eliminated with the addition of 4 mM ascorbic acid at the end of the enzymatic reaction at 4°C (Supplementary Figure S5A). Fitting the concentration of the product at increasing concentrations of diclofenac leads to a Michaelis-Menten curve from which a K_M of 49.6 ± 6.3 μM and a k_{cat} of 0.06 ± 0.01 min⁻¹ were calculated (Figure 6D). The turnover was further increased to 0.19 ± 0.01 min⁻¹ by optimising the concentration of H₂O₂ (0.25 mM), temperature (30°C) and incubation time (30 min). Detection of the product was only possible in the presence of both cytochrome P450 and H₂O₂ and at the same retention time (7.99-8.01 min) of a 5-hydroxydiclofenac standard (Supplementary Figure S5B), confirming that this subfamily is particularly prone to conversion of diclofenac and through peroxide shunt. Thus, P450 116B5hd may be another good target for large scale biotransformation in order to increase the yield to a satisfying amount of product.

Conclusions

This work demonstrates that the particular features of P450 116B5 heme domain, i.e. its high reduction potential and unusually high tolerance to H₂O₂, makes this enzyme compatible with a peroxide shunt driven catalysis. The absence of its physiological reductase is an advantage for this type of enzyme, as it simplifies its purification, increases expression yield and reduces the cost of exploitation as a biocatalyst in that no NADPH is needed.

H₂O₂ driven catalysis by P450 116B5hd was demonstrated by conversion of several substrates such as aromatic compounds as well as known drugs. Further developments using whole cells expressing the enzyme for production of human drug metabolites can be envisaged [47]. Finally, even if P450s show limitation in catalysis [48], peroxygenase and

peroxygenase-like P450s catalyse interesting reactions with high regio- and stereo-selectivity with consequent high biotechnological impact.

Funding

No specific grants were received for this work.

Declaration of Interest

Declaration of interest: none.

Figure and Table Legends

Figure 1: A. Amino acid sequence of P450 116B5hd with secondary structure prediction. The first 452 aa are depicted and the secondary structure prediction is shown as follows: red tubes: α -helices, green arrows: β -sheets, small blue tubes: random coils. Question marks indicate regions of high disorder predicted as a domain boundary. The conserved molecular oxygen and heme binding sites are marked with single underline and open circles, respectively. The conserved cysteine residue that provides the fifth ligand to the heme iron is marked by an asterisk. B. Constructs scheme of P450 116B5hd. Three different PCR constructs including a 6x histidine tag were amplified from C116B5 full length and inserted into a pET-30a (+) vector shown below between NdeI and EcoRI restriction sites. C. 12% SDS-PAGE gel. P450 116B5hd (constructs of 442 aa) is shown in its purified form at 51.7 Kda: lane 1, Molecular weight marker; lane 2, 1 μ g protein after elution from nickel column; lane 3, 1 μ g protein eluted from SEC column. Sizes of marker bands indicated.

Figure 2: Spectroscopic features of P450 116B5hd. A. Absorption spectra of purified P450 116B5hd. Spectrum of the ferric (dotted line), sodium dithionite-reduced ferrous (dashed line), and ferrous-CO complexes of purified protein (pointed line) in 50 mM potassium phosphate buffer (pH 6.8), 10% glycerol. B. Absorption spectra of oxidized P450 116B5hd (black line) and ligand bound form with diclofenac (dotted line) and ketoconazole (dashed line). Inset: difference spectra of palmitoleic-bound minus -free enzyme (top spectrum) and ketoconazole-bound minus -free enzyme (bottom spectrum).

Figure 3: A. DSC profiles of P450 116B5hd 10 μ M at different pH values. Temperature gradient: 25-90°C, 90° C/h scan rate, 10 min pre-scan equilibration at pH 5: black line, pH=5.5 dashed line, pH=6.2 grey line, pH=6.8 pointed line, pH=7.4 grey dashed line, pH=8 black bold line. B. Activity at different pH values. Conversion of *p*-nitrophenol to *p*-nitrocatechol at different pH values for 30 min over 30°C. C. Spectro-electrochemical titrations of P450 116B5hd in the absence (filled circles) and presence of ketoconazole 50 μ M (empty squares) or diclofenac 100 μ M (empty triangles). Spectra were recorded every 5 min and the normalized reduced form of the enzyme at 550 nm wavelength is plotted against the measured potential (NHE reference electrode/Volt). Data are fitted using the Nernst function to define a midpoint potential.

Figure 4: P450 BMP and P450 116B5hd H₂O₂ resistance comparison. A. P450 BMP UV-Vis spectrum after the addition of 1 mM H₂O₂. Protein concentration was 2.5 μ M. B. P450 116B5hd spectrum after the addition of 1 mM H₂O₂. Protein concentration was 2.5 μ M. Both spectra show heme absorbance decrease due to H₂O₂-mediated oxidation of the prosthetic group in 30 min at 15°C. C. 419 nm decay in 30 min of BMP WT in KPi with 0.25 mM H₂O₂ (empty circles), 2 mM (filled triangles) and 5 mM H₂O₂ (empty triangles) and a control without H₂O₂ (filled circles). D. 419 nm decay in 30 min of P450 116B5hd in KPi with 0.25 mM H₂O₂ (empty circles), 2 mM (black triangles) and 5 mM H₂O₂ (empty triangles) and a control without H₂O₂ (filled circles).

Figure 5: Comparison of conversion of *p*-nitrophenol into *p*-nitrocatechol by P450 BM3, BMP and P450 116B5hd. A. Reaction of P450 BM3 using 1mM NADPH; B. Reaction of BMP using 400 μ M H₂O₂ ; C. P450 116B5hd using 400 μ M hydrogen peroxide. All

reactions were run for 30 min at 30°C, 0.1 mM Kpi pH 8 for P450 BM3 and BMP, and 50 mM KPi pH 6.8 for P450 116B5hd. For each enzyme, three concentrations of *p*-nitrocatechol were used: 0.2 (white), 0.6 (light grey) and 1.6 mM (dark grey)

Figure 6: Michaelis Menten curves for different substrates. A. Curve fitting for *p*-nitrophenol conversion. Reactions performed for 30 min at 30°C with 600 μM H_2O_2 . B. Amplex red product curve fitting in presence of 1 μM of protein with 500 μM H_2O_2 . C. 5OH-diclofenac product curve fitting in presence of 1 μM of protein with 500 μM H_2O_2 . D. N-desmethyl tamoxifen curve fitting in presence of 1 μM of protein with 500 μM H_2O_2 .

Table 1: Thermal stability as a function of pH. Melting temperature (T_M) values and their related enthalpy (ΔH_{cal}) at different pH were calculated from fitting the differential scanning calorimetry curves of Figure 3A.

Table 2: Substrate and inhibitors screening. Molecules tested and type of shift observed in the spectrum of P450 116B5hd.

Table 3: P450 BMP and P450 116B5hd stability to hydrogen peroxide. Rate constants (k) of the decay of the Soret peak and percentage of loss of A_{419} for BMP and P450 116B5hd in the presence of increasing concentrations of H_2O_2 .

Table 4: Reactions performed by P450 116B5hd via the peroxide shunt. A) hydroxylation of *p*-nitrophenol to *p*-nitrocatechol; B) conversion of 10-acetyl-3,7-dihydroxyphenoxazine (Amplex red) to resorufin; C) oxidation of the benzidine derivative 3,5,3',5'-tetramethylbenzidine (TMB) to its diimine oxidized product; D) N-demethylation of tamoxifen into desmethyl-tamoxifen; E) hydroxylation of diclofenac into 5-hydroxydiclofenac.

References

- [1] Omura T, Sato RJ. The carbon monoxide-binding pigment of liver microsomes. *J Biol Chem* 1964;239:2370–2378.
- [2] Ciaramella A, Minerdi D, Gilardi, G. Catalytically self-sufficient cytochromes P450 for green production of fine chemicals. *Rend Linc Sci Fis Nat* 2017;28:169–181. DOI: 10.1007/s12210-016-0581-z
- [3] Yun CH, Kim KH, Kim DH, Jung HC, Pan JG. The bacterial P450 BM3: a prototype for a biocatalyst with human P450 activities. *Trends Biotechnol* 2007;25(7):289–298.
- [4] Miura Y, Fulco AJ. (Ω -2) hydroxylation of fatty acids by a soluble system from *Bacillus megaterium*. *J Biol Chem* 1974;249:1880–1888.
- [5] Munro AW, Leys DG, McLean KJ, Marshall KR, Ost TW, Daff S, et al. P450 BM3: the very model of a modern flavocytochrome. *Trends Biochem Sci* 2002;27(5):250–257.
- [6] Sadeghi SJ, Gilardi G. Chimeric P450 enzymes: activity of artificial redox fusions driven by different reductases for biotechnological applications. *Biotechnol Appl Bioc* 2013;60(1):102–110.
- [7] Gilardi G, Meharena YT, Tsotsou GE, Sadeghi SJ, Fairhead M, Giannini S. Molecular Lego: design of molecular assemblies of P450 enzymes for nanobiotechnology. *Biosens Bioelectron* 2002;17(1-2):133–145.
- [8] Bernhardt R. Cytochromes P450 as versatile biocatalysts. *J Biotechnol* 2006;124(1):128–145.
- [9] Urlacher VB, Eiben S. Cytochrome P450 monooxygenases: perspectives for synthetic application. *Trends Biotechnol* 2006;24(7):324–330.
- [10] Hrycay EG, Bandiera SM. Monooxygenase, Peroxidase and Peroxygenase Properties and Mechanisms of Cytochrome P450 Springer-Verlag Berlin, 2015, p. 16-41;
- [11] Matsunaga I, Yamada M, Kusone E, Miki T, Ichihara K. Further characterization of hydrogen peroxide-dependent fatty acid α -hydroxylase from *Sphingomonas paucimobilis*. *J Biochem* 1998;124:105-110.
- [12] Matsunaga I, Ueda A, Fujiwara N, Sumimoto T, and Ichihara K. Characterization of the ybdT gene product of *Bacillus subtilis*: novel fatty acid β -hydroxylating cytochrome P450. *Lipids* 1999;34(8):841–846.
- [13] Girhard M., Schuster S., Dietrich M., Durre P. and Urlacher VB. Cytochrome P450 monooxygenase from *Clostridium acetobutylicum*: A new α -fatty acid hydroxylase. *Biochem Biophys Res Commun* 2007;362(1):114-119.

- [14] Shoji O, Fujishiro T, Nakajima H, Kim M, Nagano S, Shiro Y et al. Hydrogen Peroxide Dependent Monooxygenations by Tricking the Substrate Recognition of Cytochrome P450_{BSβ}. *Angew Chem Int Edit* 2007;46(20):3656–3659.
- [15] Shoji O, Fujishiro T, Nishio K, Kano Y, Kimoto H, Chien SC, et al.. A substrate-binding mimic of H₂O₂-dependent cytochrome P450 produced by one-point mutagenesis and peroxygenation of non-native substrates. *Catal Sci Tech* 2016;6:5806-5811. DOI: 10.1039/C6CY00630B
- [16] Minerdi D., Sadeghi SJ, Di Nardo G, Rua F, Castrignanò S, Allegra P, et al.. CYP116B5: a new class VII catalytically self-sufficient cytochrome P450 from *Acinetobacter radioresistens* that enables growth on alkanes: Oxidation of n -alkanes by a novel self-sufficient bacterial cytochrome P450. *Mol Microbiol* 2015;95(3):539–554.
- [17] Pessione, E., and Giunta, C. *Acinetobacter radioresistens* metabolizing aromatic compounds. Biochemical and microbiological characterization of the strain. *Microbios* 1997; 89:105–117.
- [18] Minerdi, D., Zgrablic, I., Castrignanò, S., Catucci, G., Medana, C., Terlizzi, M.E., et al. *Escherichia coli* overexpressing a Baeyer-Villiger monooxygenase from *Acinetobacter radioresistens* become resistant to Imipenem. *Antimicrob Agents Chemother* 2016;60:64-74.
- [19] Klenk JM, Nebel BA, Porter JL, Kulig JK, Hussain SA, Richter SM, et al. The self-sufficient P450 RhF expressed in a whole cell system selectively catalyses the 5-hydroxylation of diclofenac. *Biotechnol J* 2017;12(3).
- [20] Munro AW, Lindsay JG, Coggins JR, Kelly SM, and Price NC. Analysis of the structural stability of the multidomain enzyme flavocytochrome P-450 BM3. *Biochim Biophys Acta*. 1996;1296:127–37.
- [21] Jones DT. Protein secondary structure prediction based on position-specific scoring matrices. *J Mol Biol* 1999;292:195-202.
- [22] Li H, Poulos TL. The structure of the cytochrome p450BM-3 haem domain complexed with the fatty acid substrate, palmitoleic acid. *Nat Struct Mol Biol* 1997;4:140–146.
- [23] Gao C, Catucci G, Castrignanò S, Gilardi G. and Sadeghi SJ. Inactivation mechanism of N61S mutant of human FMO3 towards trimethylamine. *Sci Rep*. 2017;7(1):14668.
- [24] Fairhead M, Giannini S, Gillam EMJ and Gilardi G. Functional characterisation of an engineered multidomain human P450 2E1 by molecular Lego. *J Biol Inorg Chem* 2005;10(8): 842–853.
- [25] Joo, J, Wu Z, Lee B, Shon JC, Lee T, Lee I, et al. In vitro metabolism of an estrogen-related receptor γ modulator, GSK5182, by human liver microsomes and recombinant cytochrome P450s. *Biopharm Drug Dispos* 2015;36(3):163–173.
- [26] Tavanti, M., Porter, J.L., Levy, C.W., Gómez Castellanos, J.R., Flitsch, S.L., Turner,

N.J. The crystal structure of P450-TT heme-domain provides the first structural insights into the versatile class VII P450s. *Biochem and Biophys Res Commun* 2018;501(4):846–850.

[27] Warman AJ, Robinson JW, Luciakova D, Lawrence AD, Marshall KR, Warren MJ, et al. Characterization of *Cupriavidus metallidurans* CYP116B1 - A thiocarbamate herbicide oxygenating P450-phthalate dioxygenase reductase fusion protein: Biochemical analysis of CYP116B1. *FEBS J* 2012;279(9):1675–1693.

[28] Raag R, Li H, Jones BC, Poulos TL. Inhibitor-induced conformational change in cytochrome P450cam. *Biochemistry* 1993;32(17):4571-4578.

[29] Conner KP, Cruce AA, Krzyaniak MD, Schimpf AM, Frank DJ, Ortiz de Montellano P, et al. Drug modulation of water-heme interactions in low-spin P450 complexes of CYP2C9d and CYP125A1. *Biochemistry* 2015;54(5):1198-207

[30] Dutton L. Redox potentiometry: Determination of midpoint potentials of oxidation-reduction components of biological electron-transfer systems. in *Methods Enzymol* 1978;54: 411–435. THIS REFERENCE IS 40 YEARS OLD. IS THERE A MORE RECENT ONE?

[31] Belcher J, McLean KJ, Matthews S, Woodward LS, Fisher K, Rigby SEJ, et al. Structure and Biochemical Properties of the Alkene Producing Cytochrome P450 OleT_{JE} (CYP152L1) from the *Jeotgalicoccus* sp. 8456 Bacterium. *J Biol Chem* 2014; 289(10):6535–6550.

[32] Albertolle MW, Kim D, Nagy LD, Yun CH, Pozzi A, Savas Ü, et al. Heme-Thiolate Sulfenylation of Human Cytochrome P450 4A11 Functions as a Redox Switch for Catalytic Inhibition. *J Biol Chem* 2017;292(27):11230-11242.

[33] Matthews S, Tee KL, Rattray NJ, McLean KJ, Leys D, Parker DA, et al. Production of alkenes and novel secondary products by P450 OleT_{JE} using novel H₂O₂-generating fusion protein systems. *FEBS Lett* 2017;591(5):737–750.

[34] Salazar O, Cirino PC, Arnold FH. Thermostabilization of a Cytochrome P450 Peroxygenase. *ChemBioChem* 2003;4(9):891–893.

[35] Li Y, Drummond DA, Sawayama AM, Snow CD, Bloom JD, Arnold FH. A diverse family of thermostable cytochrome P450s created by recombination of stabilizing fragments. *Nat Biotechnol* 2007;25(9):1051–1056.

[36] Li QS, Ogawa J, Shimizu S. Critical role of the residue size at position 87 in H₂O₂-dependent substrate hydroxylation activity and H₂O₂ inactivation of cytochrome P450BM-3. *Biochem Biophys Res Commun* 2001;280(5):1258-1261.

[37] Arnao MB, Acosta M, del Río JA, Varón R, García-Cánovas F. A kinetic study on the suicide inactivation of peroxidase by hydrogen peroxide. *Biochim Biophys Acta* 1990; 1041(1):43-7.

- [38] Nakajima R, Yamazaki I. The mechanism of oxyperoxidase formation from ferryl peroxidase and hydrogen peroxide. *J Biol Chem* 1987;262(6):2576-81.
- [39] Cirino PC, Arnold FH. A Self-Sufficient Peroxide-Driven Hydroxylation Biocatalyst. *Angew Chem Int Edit* 2003;42(28):3299–3301.
- [40] Ortiz de Montellano PR. *Cytochrome P450. Structure, mechanism, and biochemistry.* 4th ed. New York. Springer; 2015.
- [41] Di Nardo G, Fantuzzi A, Sideri A, Panicco P, Sassone C, Giunta C, et al. Wild-type CYP102A1 as a biocatalyst: turnover of drugs usually metabolised by human liver enzymes. *J Biol Inorg Chem* 2007;12(3):313-323.
- [42] Catucci G, Zgrablic I, Lanciani F, Valetti F, Minerdi D, Ballou DP, et al. Characterization of a new Baeyer-Villiger monooxygenase and conversion to a solely N-or S-oxidizing enzyme by a single R292 mutation. *Biochim Biophys Acta, Proteins Proteomics* 2016;1864(9):1177–1187.
- [43] Rabe KS, Erkelenz M, Kiko K, Niemeyer CM. Peroxidase activity of bacterial cytochrome P450 enzymes: Modulation by fatty acids and organic solvents. *Biotechnology J* 2010;5(8):891–899.
- [44] Matsunaga I, Sumimoto T, Ayata M, Ogura H. Functional modulation of a peroxygenase cytochrome P450: novel insight into the mechanisms of peroxygenase and peroxidase enzymes. *FEBS Lett* 2002;528:90–94.
- [45] Tavanti M, Porter JL, Sabatini S, Turner NJ, Flitsch SL. Panel of New Thermostable CYP116B Self-Sufficient Cytochrome P450 Monooxygenases that Catalyze C–H Activation with a Diverse Substrate Scope. *Chem Cat Chem* 2018;10(5):1042-1051.
- [46] Huber C, Preis M, Harvey PJ, Grosse S, Letzel T, Schröder P. Emerging pollutants and plants – Metabolic activation of diclofenac by peroxidases. *Chemosphere* 2016;146:435–441.
- [47] Poraj-Kobielska M, Atzrodt, J, Holla W, Sandvoss M, Gröbe G, Scheibner K, et al. Preparation of labeled human drug metabolites and drug-drug interaction-probes with fungal peroxygenases. *J Labelled Comp Radiopharm* 2013;56(9-10):513–519.
- [48] Bernhardt R, Urlacher VB. Cytochromes P450 as promising catalysts for biotechnological application: chances and limitations. *Appl Microbiol Biotechnol* 2014;98(14): 6185–6203.

**Peroxide-driven catalysis of the heme domain of *A. radioresistens*
cytochrome P450 116B5 for sustainable aromatic rings oxidation
and drug metabolites production**

Alberto Ciaramella, Gianluca Catucci, Giovanna Di Nardo, Sheila J. Sadeghi
and Gianfranco Gilardi*

Department of Life Sciences and Systems Biology,
University of Torino, Via Accademia Albertina 13, 10123 Torino, Italy.

* Address correspondence to:

Gianfranco Gilardi
gianfranco.gilardi@unito.it

Tables

Table 1: Thermal stability as a function of pH. Melting temperature (T_M) values and their related enthalpy (ΔH_{cal}) at different pH were calculated from fitting the differential scanning calorimetry curves of Figure 3A.

pH	T_{M1} (°C)	ΔH_{cal1} (KJ/mol)	T_{M2} (°C)	ΔH_{cal2} (KJ/mol)
5.0	44.4	150.0	38.8	197.0
5.5	44.8	260.0	40.2	191.0
6.2	49.9	466.1	---	---
6.8	48.2	502.0	---	---
7.4	50.1	410.7	---	---
8.0	51.0	127.7	46	168.4

Table 2: Substrate and inhibitors screening. Molecules tested and type of shift observed in the spectrum of P450 116B5hd.

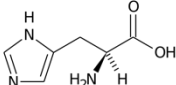
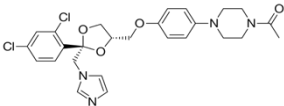
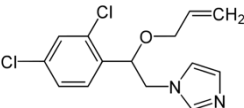
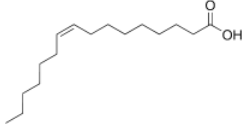
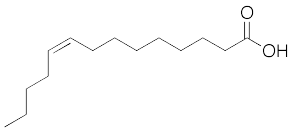
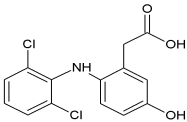
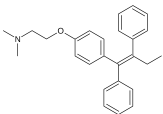
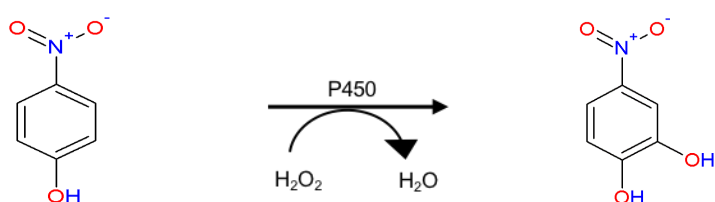
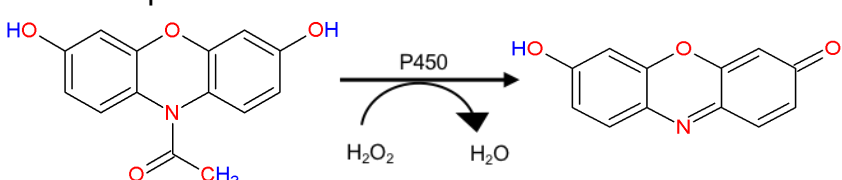
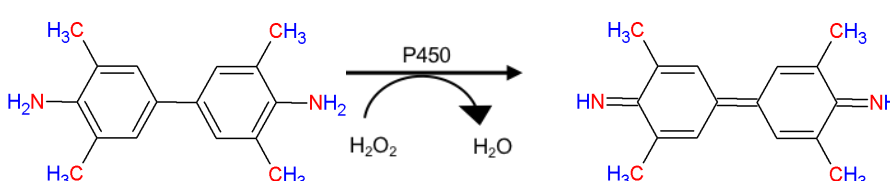
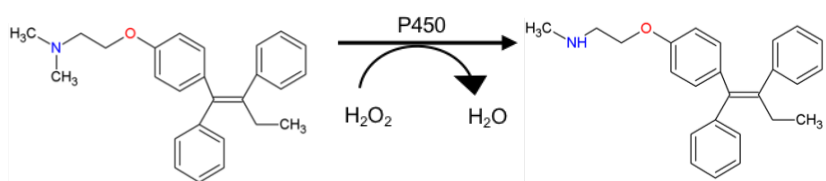
Name	Ligand	Type of shift observed on the Soret peak at 419 nm
Imidazole		Type II
Histidine		Type II
Ketoconazole		Type II
Imazalil		Type II
Palmitoleic Acid		Small Type I
Myristoleic Acid		Small Type I
Diclofenac		Small Type I
Tamoxifen		No shift

Table 3: P450 BMP and P450 116B5hd stability to hydrogen peroxide. Rate constants (k) of the decay of the Soret peak and percentage of loss of A₄₁₉ for BMP and P450 116B5hd in the presence of increasing concentrations of H₂O₂.

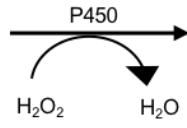
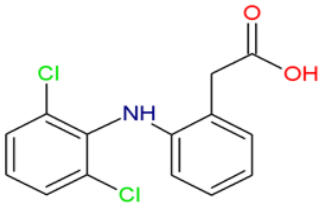
H ₂ O ₂ concentration	P450 BMP		P450 116B5hd	
	k (s ⁻¹)	% loss of A ₄₁₉	k (s ⁻¹)	% loss of A ₄₁₉
0 mM	---	3.5 ± 2.4	---	0 ± 0.8
0.25 mM	0.0274	58.2 ± 3.9	---	0.7 ± 1.8
1 mM	0.0591	64.0 ± 2.8	---	4.1 ± 0.9
2 mM	0.1179	73.2 ± 7.7	0.0024	7.2 ± 1.9
3 mM	0.1493	83.3 ± 0.6	0.0034	7.1 ± 2.9
4 mM	0.2504	81.8 ± 0.8	0.0042	5.1 ± 1.9
5 mM	0.4056	82.8 ± 1.6	0.0051	10.2 ± 0.8

Table 4: Reactions performed by P450 116B5hd via the peroxide shunt. A) hydroxylation of *p*-nitrophenol to *p*-nitrocatechol; B) conversion of 10-acetyl-3,7-dihydroxyphenoxazine (Amplex red) to resorufin; C) oxidation of the benzidine derivative 3,5,3',5'-tetramethylbenzidine (TMB) to its diimine oxidized product; D) N-demetylation of tamoxifen into desmethyl-tamoxifen; E) hydroxylation of diclofenac into 5-hydroxydiclofenac

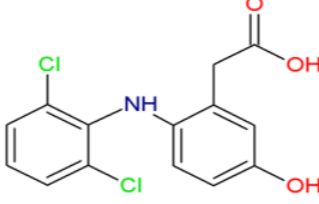
SUBSTRATE AND REACTIONS	KINETIC COSTANTS AND % TOTAL TURNOVER (TT)
<p>A <i>p</i>-nitrophenol</p>  <p><i>p</i>-nitrocatechol</p>	<p>$k_{\text{cat}} : 2.65 \pm 0.14 \text{ s}^{-1}$</p> <p>$K_{\text{M}} : 128.85 \pm 29.51 \text{ }\mu\text{M}$</p> <p>TT = 59 ± 6</p>
<p>B Amplex red</p>  <p>resorufin</p>	<p>$k_{\text{cat}} : 0.33 \pm 0.03 \text{ min}^{-1}$</p> <p>$K_{\text{M}} : 6.01 \pm 0.32 \text{ }\mu\text{M}$</p> <p>TT = 57 ± 5</p>
<p>C TMB</p>  <p>TMB ox</p>	<p>$k_{\text{cat}}, K_{\text{M}}$:and TT n.d.</p>
<p>D tamoxifen</p>  <p>desmethyl-tamoxifen</p>	<p>$k_{\text{cat}} : 0.79 \pm 0.04 \text{ min}^{-1}$</p> <p>$K_{\text{M}} : 57.20 \pm 7.90 \text{ }\mu\text{M}$</p> <p>TT = 38 ± 4</p>

E

diclofenac



5-hydroxydiclofenac



$$k_{\text{cat}} : 0.06 \pm 0.01 \text{ min}^{-1}$$

$$K_M : 49.6 \pm 6.3 \text{ } \mu\text{M}$$

$$TT = 35 \pm 5$$

**Peroxide-driven catalysis of the heme domain of *A. radioresistens* cytochrome P450 116B5 for sustainable aromatic rings
oxidation
and drug metabolites production**

Alberto Ciaramella, Gianluca Catucci, Giovanna Di Nardo, Sheila J. Sadeghi
and Gianfranco Gilardi*

Department of Life Sciences and Systems Biology,
University of Torino, Via Accademia Albertina 13, 10123 Torino, Italy.

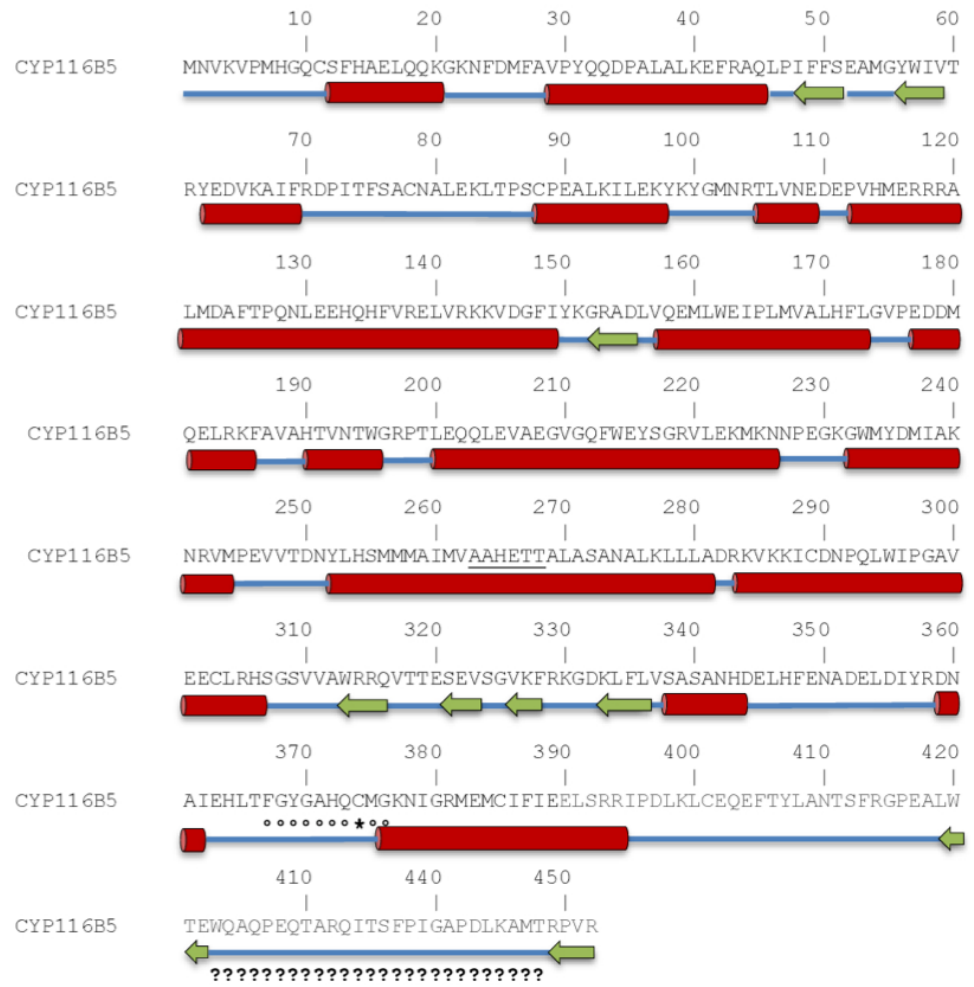
* Address correspondence to:

Gianfranco Gilardi

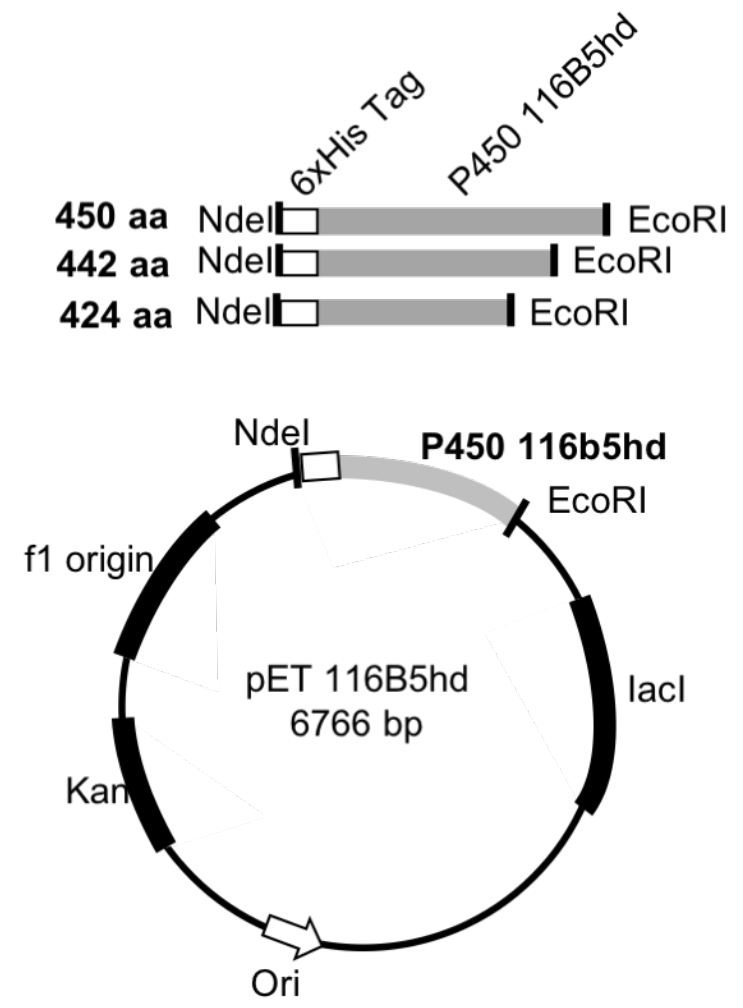
gianfranco.gilardi@unito.it

FIGURES

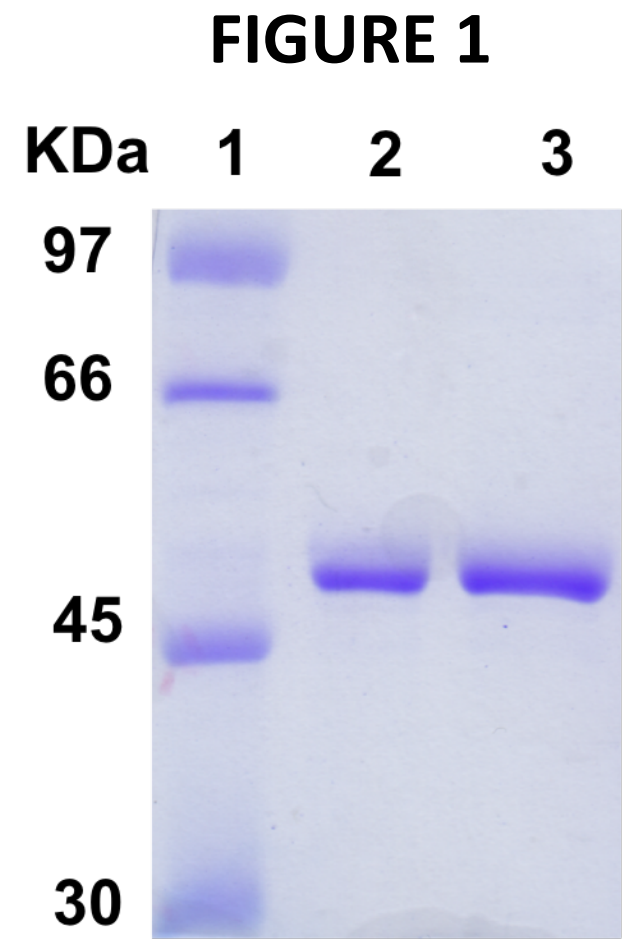
Figure 1: A. Amino acid sequence of P450 116B5hd with secondary structure prediction. The first 452 aa are depicted and the secondary structure prediction is shown as follows: red tubes: α -helices, green arrows: β -sheets, small blue tubes: random coils. Question marks indicate regions of high disorder predicted as a domain boundary. The conserved molecular oxygen and heme binding sites are marked with single underline and open circles, respectively. The conserved cysteine residue that provides the fifth ligand to the heme iron is marked by an asterisk. B. Constructs scheme of P450 116B5hd. Three different PCR constructs including a 6x histidine tag were amplified from C116B5 full length and inserted into a pET-30a (+) vector shown below between NdeI and EcoRI restriction sites. C. 12% SDS-PAGE gel. P450 116B5hd (constructs of 442 aa) is shown in its purified form at 51.7 Kda: lane 1, Molecular weight marker; lane 2, 1 μ g protein after elution from nickel column; lane 3, 1 μ g protein eluted from SEC column. Sizes of marker bands indicated.



A

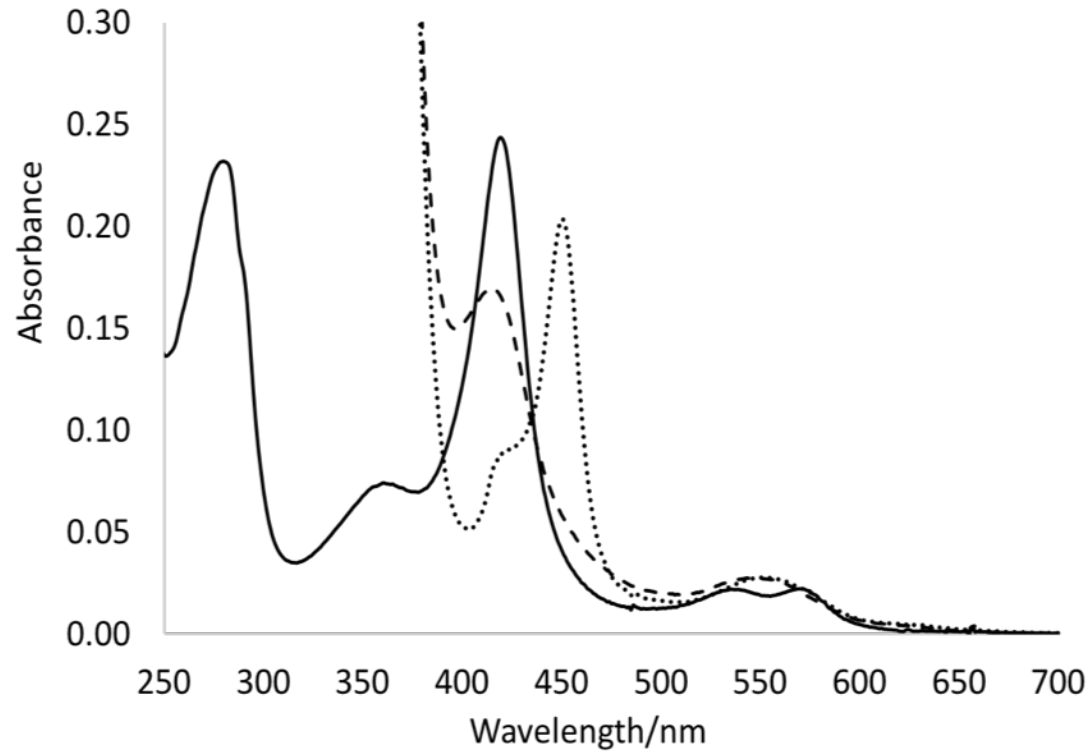


B

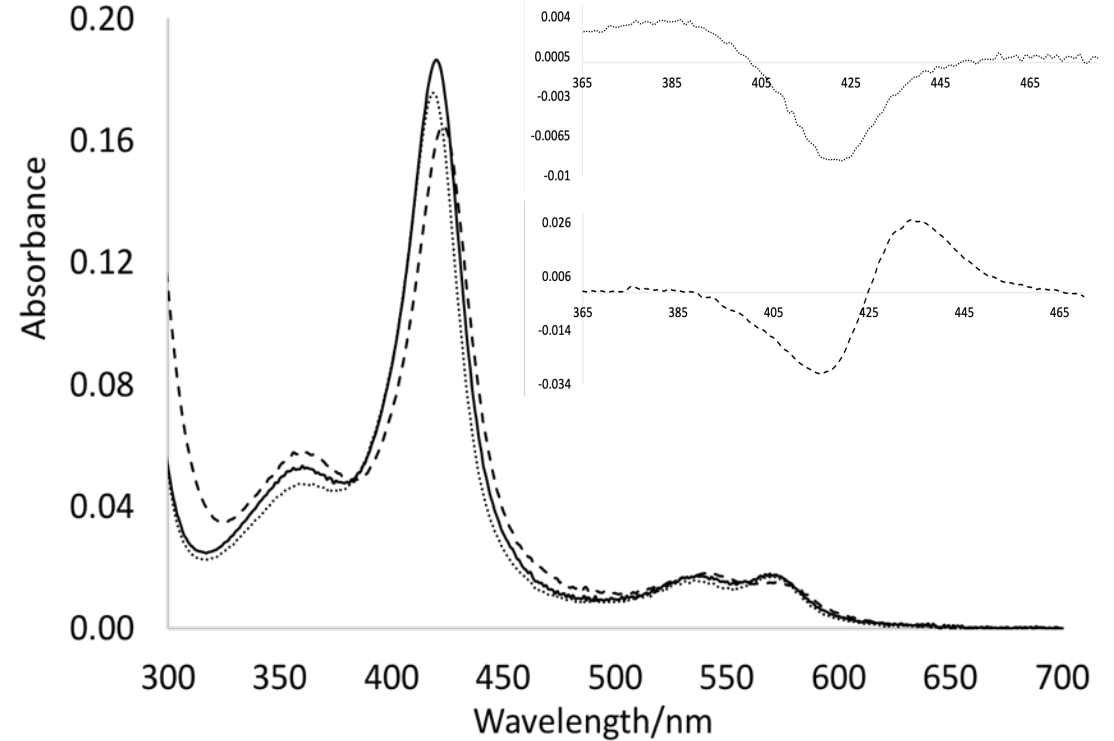


C

Figure 2: Spectroscopic features of P450 116B5hd. A. Absorption spectra of purified P450 116B5hd. Spectrum of the ferric (dotted line), sodium dithionite-reduced ferrous (dashed line), and ferrous-CO complexes of purified protein (pointed line) in 50 mM potassium phosphate buffer (pH 6.8), 10% glycerol. B. Absorption spectra of oxidized P450 116B5hd (black line) and ligand bound form with diclofenac (dotted line) and ketoconazole (dashed line). Inset: difference spectra of palmitoleic-bound minus -free enzyme (top spectrum) and ketoconazole-bound minus -free enzyme (bottom spectrum).

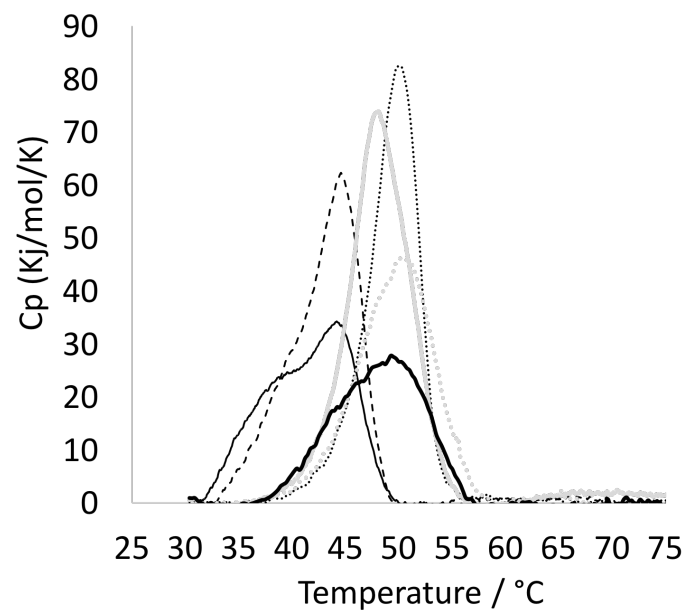


A

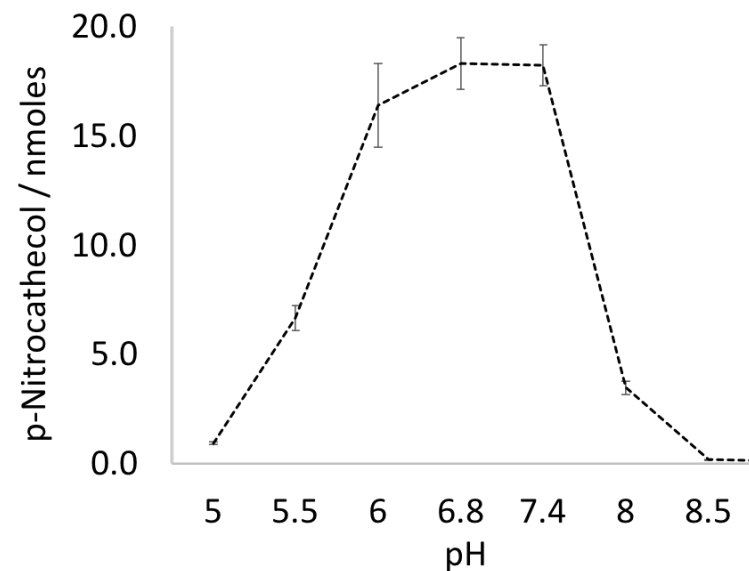


B

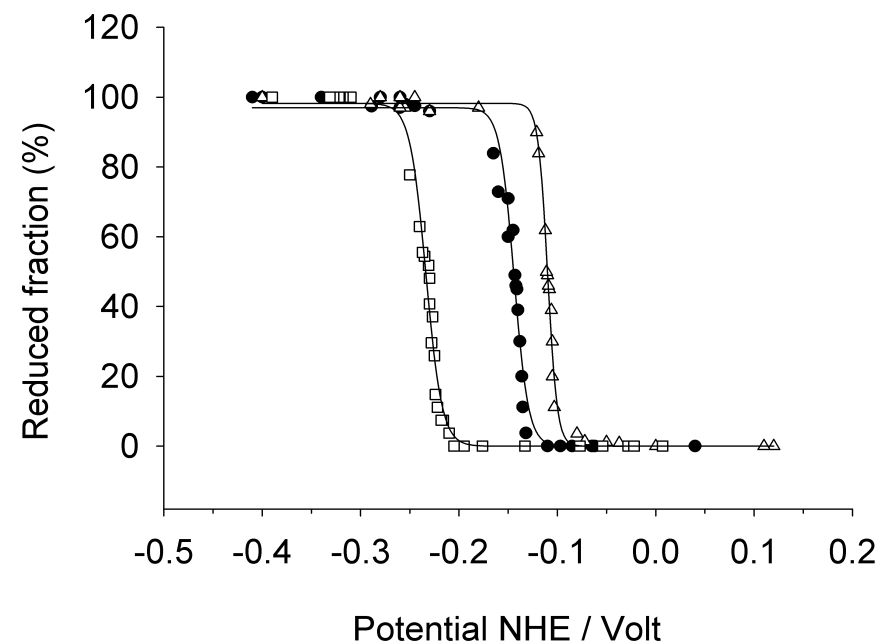
Figure 3: A. DSC profiles of P450 116B5hd 10 μM at different pH values. Temperature gradient: 25-90°C, 90°C/h scan rate, 10 min pre-scan equilibration at pH 5: black line, pH=5.5 dashed line, pH=6.2 grey line line, pH=6.8 pointed line, pH=7.4 grey dashed line, pH=8 black bold line. B. Activity at different pH values. Conversion of *p*-nitrophenol to *p*-nitrocatechol at different pH values for 30 min over 30°C. C. Spectro-electrochemical titrations of P450 116B5hd in the absence (filled circles) and presence of ketoconazole 50 μM (empty squares) or diclofenac 100 μM (empty triangles). Spectra were recorded every 5 min and the normalized reduced form of the enzyme at 550 nm wavelength is plotted against the measured potential (NHE reference electrode/Volt). Data are fitted using the Nernst function to define a midpoint potential.



A



B



C

FIGURE 3

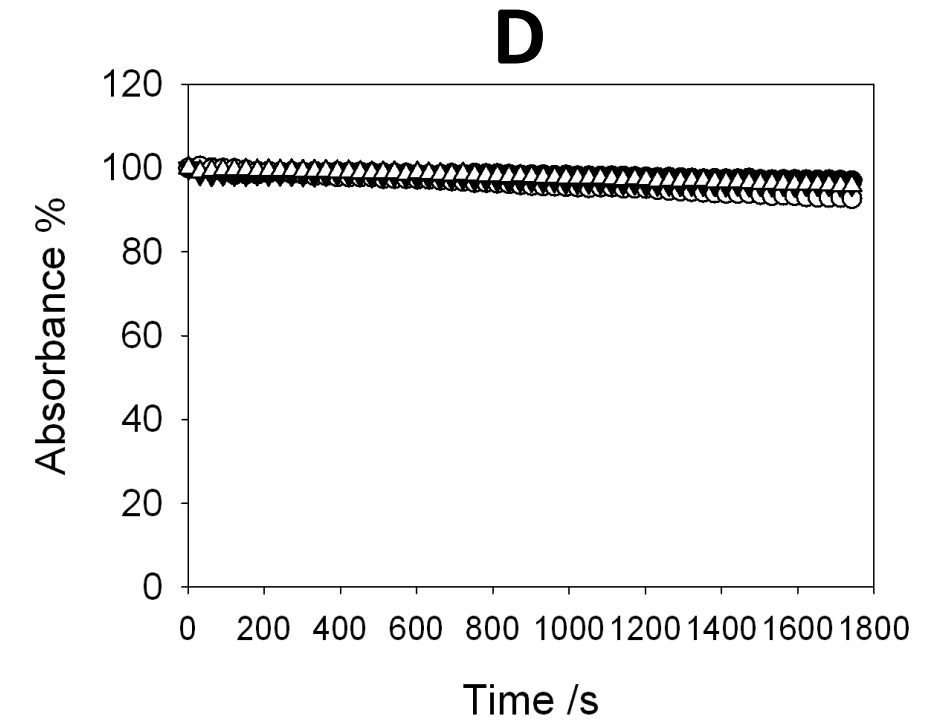
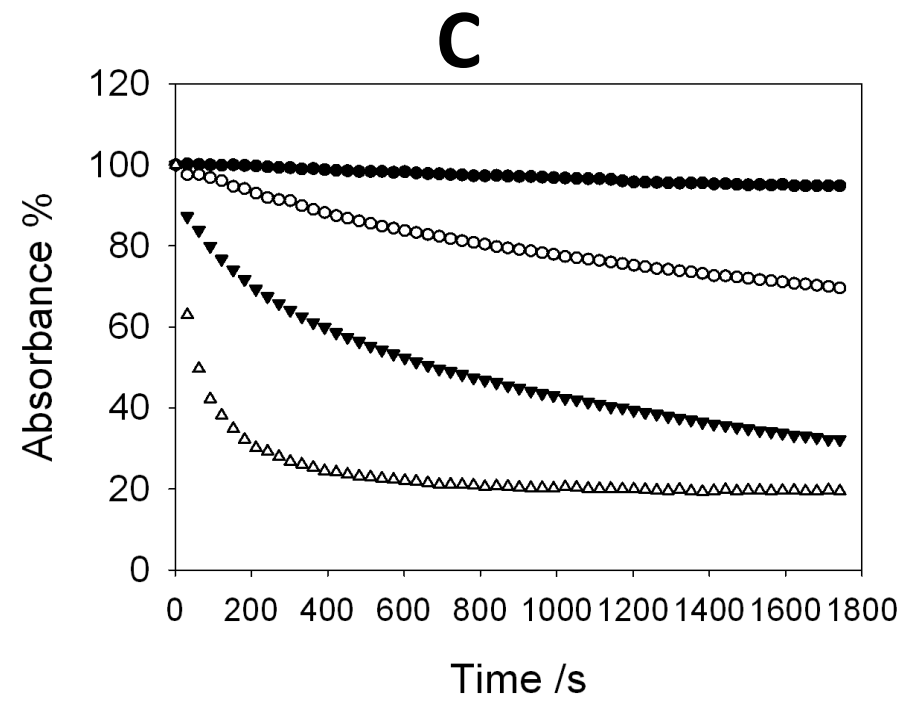
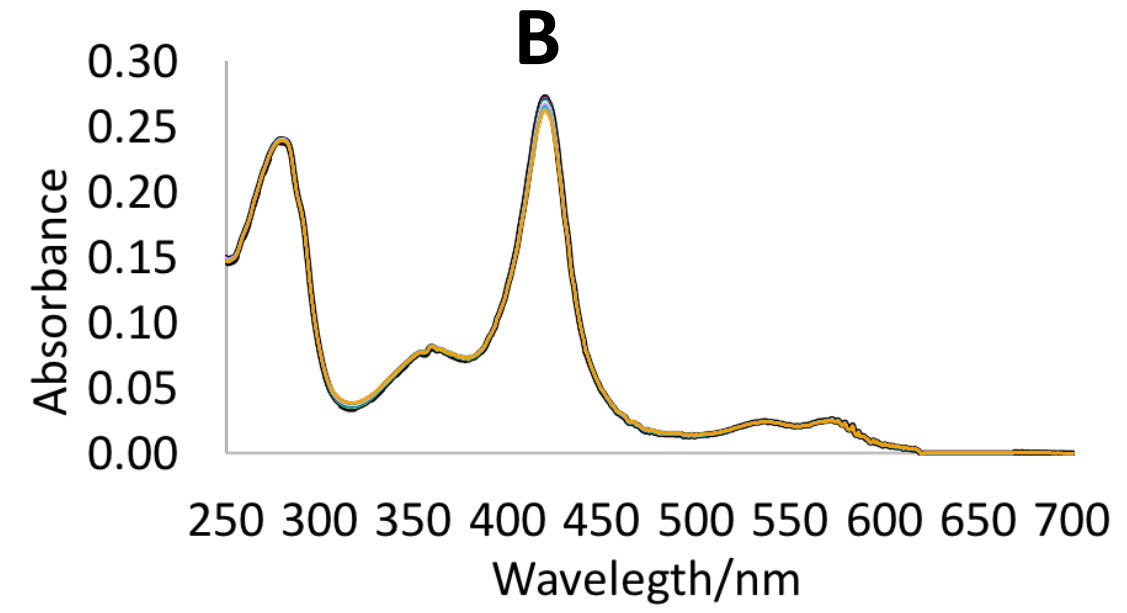
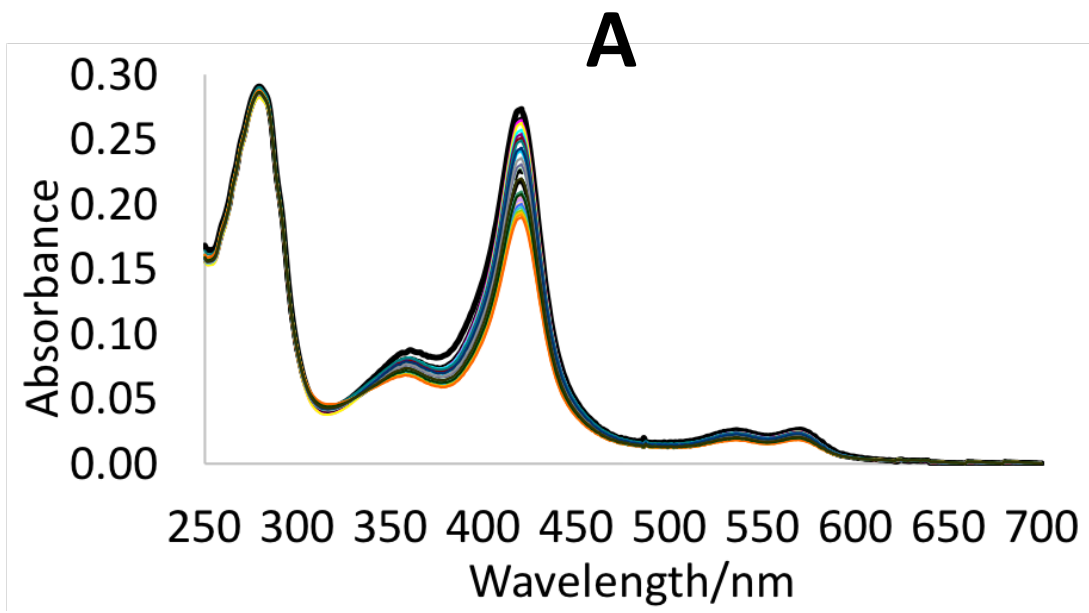


FIGURE 4

Figure 4: P450 BMP and P450 116B5hd H₂O₂ resistance comparison. A. P450 BMP UV-Vis spectrum after the addition of 1 mM H₂O₂. Protein concentration was 2.5 μM. B. P450 116B5hd spectrum after the addition of 1 mM H₂O₂. Protein concentration was 2.5 μM. Both spectra show heme absorbance decrease due to H₂O₂-mediated oxidation of the prosthetic group in 30 min at 15°C. C. 419 nm decay in 30 min of BMP WT in KPi with 0.25 mM H₂O₂ (empty circles), 2 mM (filled triangles) and 5 mM H₂O₂ (empty triangles) and a control without H₂O₂ (filled circles). D. 419 nm decay in 30 min of P450 116B5hd in KPi with 0.25 mM H₂O₂ (empty circles), 2 mM (black triangles) and 5 mM H₂O₂ (empty triangles) and a control without H₂O₂ (filled circles).

Figure 5: Comparison of conversion of *p*-nitrophenol into *p*-nitrocatechol by P450 BM3, BMP and P450 116B5hd. A. Reaction of P450 BM3 using 1mM NADPH; B. Reaction of BMP using 400 μ M H₂O₂; C. P450 116B5hd using 400 μ M hydrogen peroxide. All reactions were run for 30 min at 30°C, 0.1 mM Kpi pH 8 for P450 BM3 and BMP, and 50 mM KPi pH 6.8 for P450 116B5hd. For each enzyme, three concentrations of *p*-nitrocatechol were used: 0.2 (white), 0.6 (light grey) and 1.6 mM (dark grey)

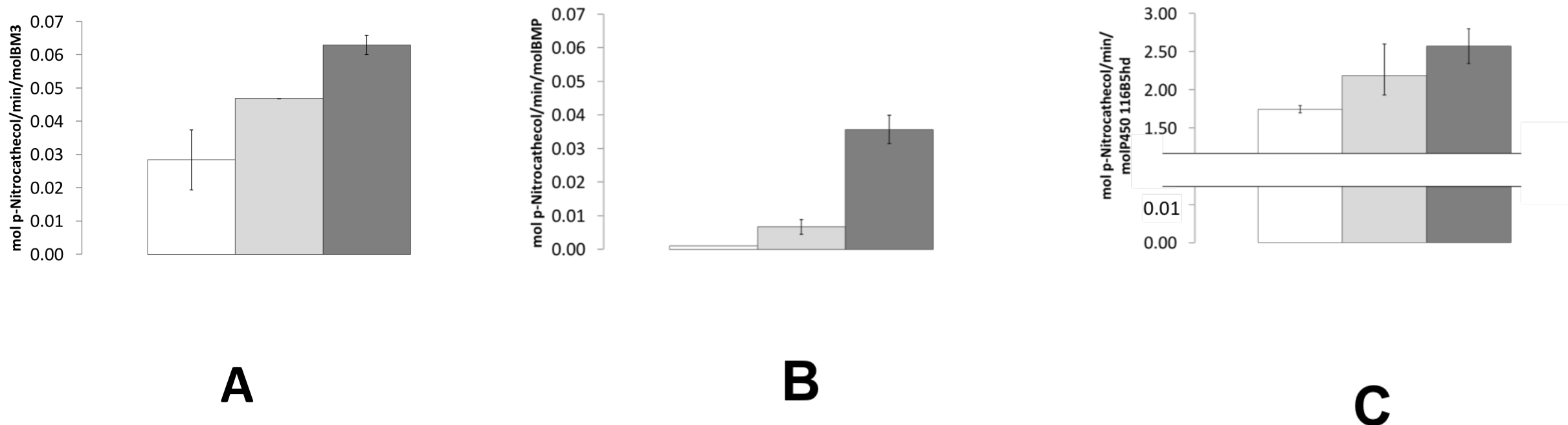


FIGURE 5

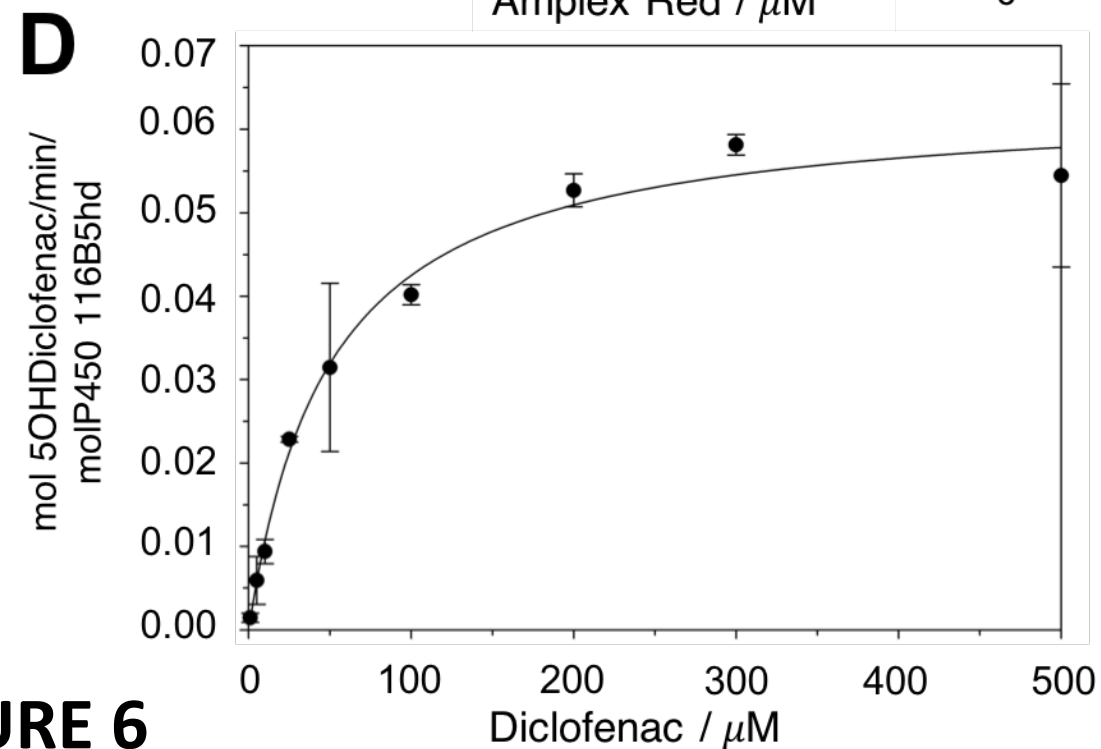
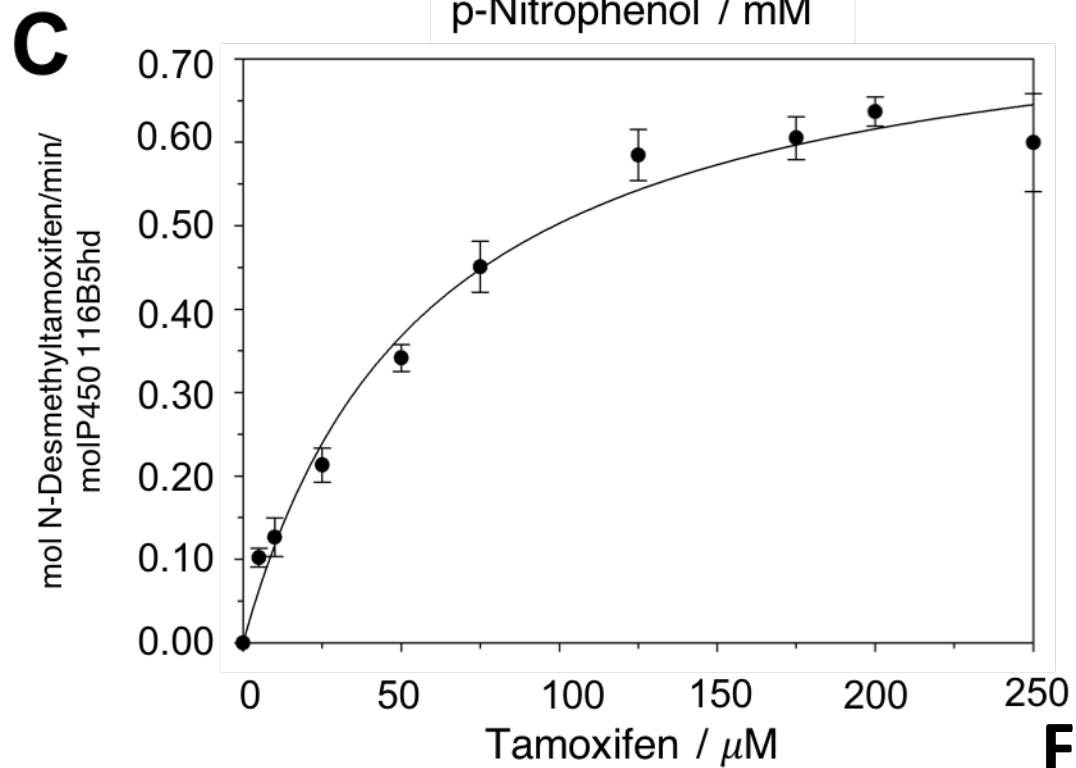
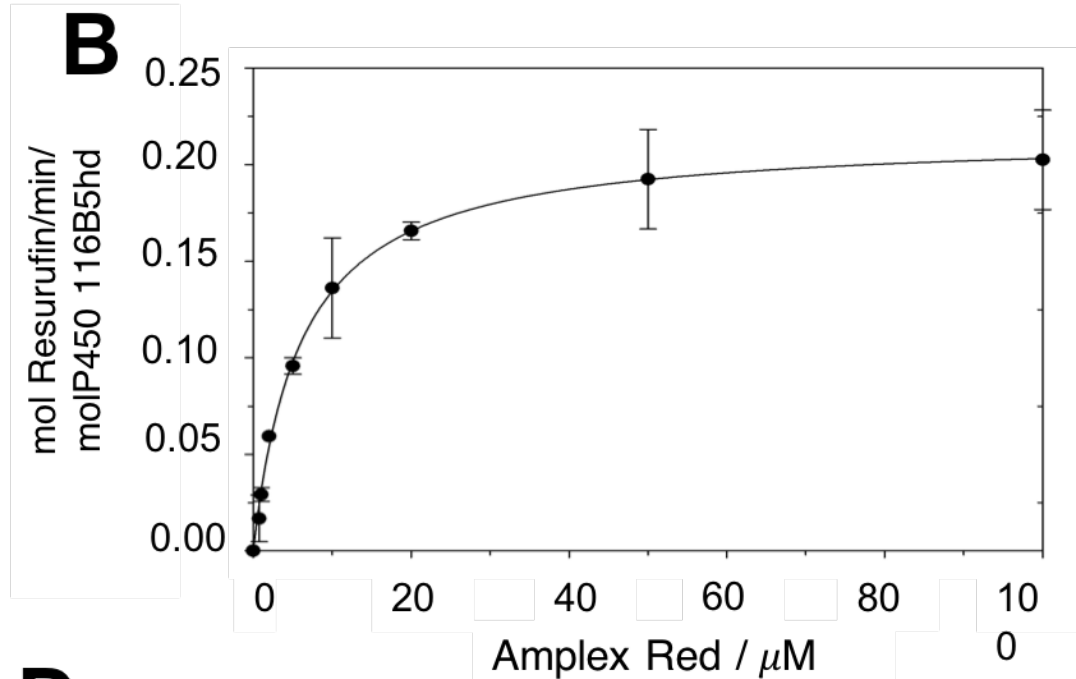
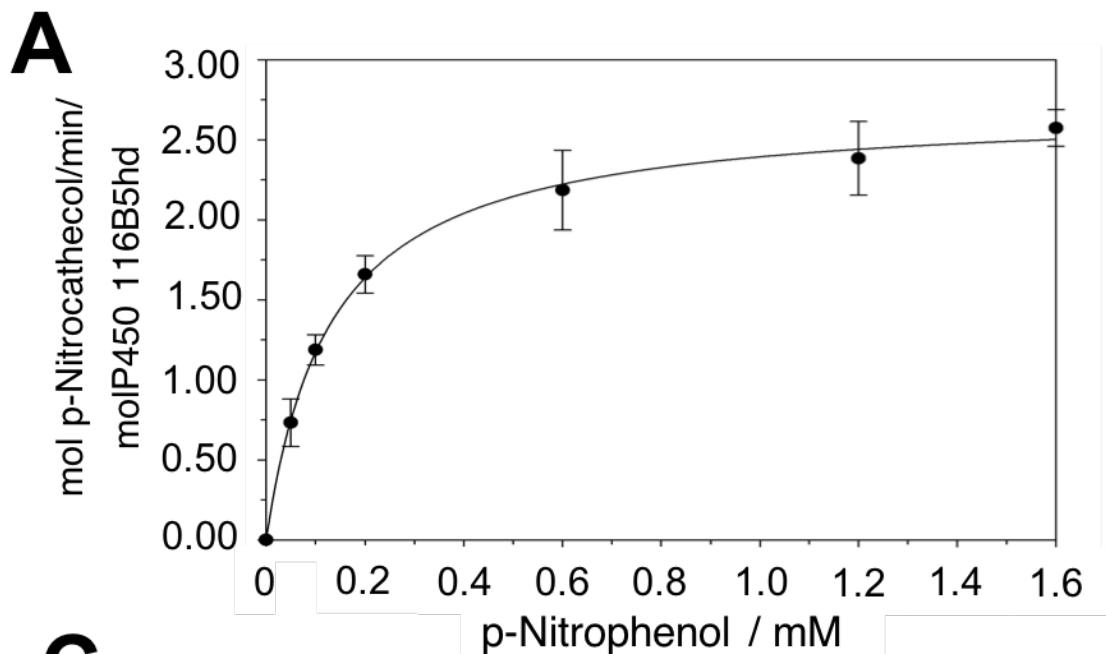


FIGURE 6

Figure 6: Michaelis Menten curves for different substrates. A. Curve fitting for p-nitrophenol conversion. Reactions performed for 30 min at 30°C with 600 μM H_2O_2 . B. Amplex red product curve fitting in presence of 1 μM of protein with 500 μM H_2O_2 . C. 5OH-diclofenac product curve fitting in presence of 1 μM of protein with 500 μM H_2O_2 . D. N-desmethyl tamoxifen curve fitting in presence of 1 μM of protein with 500 μM H_2O_2 .